SEMARAK ILMU PUBLISHING

Journal of Advanced Research in Fluid Mechanics and Thermal Sciences

Journal homepage:
https://semarakilmu.com.my/journals/index.php/fluid_mechanics_thermal_sciences/index
ISSN: 2289-7879

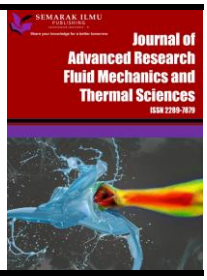

Experimental Investigation on Performance Comparison between Flat Plate and Matrix of Tubes Solar Air Heater

Munther Abdullah Mussa[1,*], Sarmad Abdul-Razzaq Rashid[2], Issam Mohammed Ali Aljubury[1]

[1] Department of Mechanical Engineering, University of Baghdad, 10071 Baghdad, Iraq
[2] Department of Chemical Engineering, University of Baghdad, 10071 Baghdad, Iraq

ARTICLE INFO

Article history:
Received 9 June 2024
Received in revised form 12 August 2024
Accepted 13 August 2024
Available online 30 October 2024

Keywords:
Matrix Tube Solar Air Heater (MTSAH); Flat Plate Solar Air Heater (FPSAH); absorber plate designs; efficiency; energy gain; solar energy

ABSTRACT

This study is a comparative study of two solar Air Heaters (SAH) having different absorber plates: the Flat Plate Solar Air Heater (FPSAH) with a flat metal plate and the Matrix Tube Solar Air Heater (MTSAH) using novel design of longitudinal circular metal tubes. The objective is to study the possible enhancement in the thermal performance of the newly designed SAH compared to the traditional one. The results clearly confirmed the priority of MTSAH over FPSAH in different properties. Compared to the FPSAH, the MTSAH showed high thermal efficiency, output power, and outlet air temperature, with decreased in heat loss. Moreover, the temperature difference between the outlet and inlet air temperatures achieved a remarkable value of 46.5°C at an inlet air mass flow rate of 0.03 kg/s for MTSAH configuration. Furthermore, the average daily efficiency of the MTSAH stands at approximately 72.55%, 85.77%, and 92.18% for air mass flow rates of 0.03, 0.05, and 0.071 kg/s, respectively. These values represent substantial enhancements of 42.25%, 50.04%, and 52.33%, respectively, compared to the FPSAH. These findings suggest new possibilities for efficient SAH designs, impacting renewable energy and sustainable heating systems. They contribute to better energy utilization from solar thermal sources, promoting sustainability.

1. Introduction

The escalating global demand for versatile energy sources has spurred scientific exploration of alternative resources. Solar energy, abundant and renewable, contrasts with finite fossil fuels. It's an inexhaustible, eco-friendly, and sustainable energy source [1,2]. A prevalent method for harnessing solar energy is through solar collectors, which efficiently convert it into thermal energy for heating applications [3,4]. One of the most common devices of solar collectors are air solar heaters [5].

Solar air heaters (SAH) come in various types, with flat plate solar air heaters (FPSAH s) being the most widely used [6]. These systems capture solar energy to produce hot air for applications like space heating, crop drying, industrial processes, timber seasoning, and water desalination [7,8]. SAHs

* *Corresponding author.*
E-mail address: munther@coeng.uobaghdad.edu.iq

https://doi.org/10.37934/arfmts.123.1.2240

are the most used instrument which characterizes by simplicity in design and low service and maintenance needs. It is used for harvesting solar energy and converts it to thermal energy by using flat plate collectors [9].

In SAHs, the absorber plate absorbs sun rays and transfers heat energy to the air by the mechanism of convective heat transfer [10]. Most solar heaters use the air as a working fluid, which is forced to flow from the ambient air through the intake port and passes above or beneath the absorber plate to gain the required heat, then the hot air is supplied to the required space [11,12]. However, the short airflow settling time and small surface area of the absorber plate reduce free convection heat transfer and due to the low thermal conductivity and heat capacity of the air, all solar air heaters (SAHs) have low thermal efficiency [13,14]. Also, due to non-uniform availability of solar radiation all FPSAHs have limited storage capabilities [15,16]. Therefore, enhancing the thermal efficiency of SAHs became an urgent challenge for researchers and they applied and suggested different modifications [17]. These modifications comprise methods leading to the maximized area of heat transfer between the air and the absorber plate and increase the overall heat transfer coefficient [18,19]. Introducing different shapes of corrugated absorber plates, extended surfaces, ribs, artificial roughness to increase the area of heat transfer, besides enhancing the turbulence in the solar air duct [6,20]. Also, phase change material, double-flow passages, packed beds, and thermal storage units either directly or indirectly merged with SAHs are some of the new techniques to augment the thermal efficiency of SAH [21,22].

Many articles had been published theoretically or experimentally with different innovative idea to increase the thermal efficiency of the SAHs. These included novel designs with heat transfer enhancers to reduce energy losses and the implementation of a dual-pass airflow system, both above and below the absorber plate, to mitigate top-side heat loss and enhance thermal performance [23-25].

Heydari and Mesgarpour [26] studied a unique SAH design consist of a double-pass design and a helical channel absorption plate. Due to the large area of the absorber surface, this design showed a high increase in thermal efficiency reached approximately 75% compared to FPSAH.

Hassan *et al.,* [27] compared the performance of a new SAH with a cylindrical absorption surface with a traditional FPSAH. The new design, consisting of an absorber with adjacent tubes longitudinally in the direction of flow, showed outstanding performance compared to the traditional FPSAH. Thermal efficiency, useful energy, outlet air temperature, and heat loss were much better than those of the traditional FPSAH. Interestingly, these improvements were more noticeable at low values of air flow rates. These results gave incentive that these designs are considered promising in terms of reducing costs and increasing the effectiveness of solar air heaters.

Abo-Elfadl *et al.,* [28] studied a new design consisting of a new single pass convex SAH and compared its thermal and hydraulic performance with the similar conventional FPSAH. The results showed that at an air mass flow rate of 0.025 kg/s, the improvement in thermal efficiency of the convex heater reached 133%.

Hedau and Singal [29] studied a double-pass SAH with thermal energy storage using phase change materials (PCMs). Their study focused on the thermal performance of the system. The outcomes of the investigation confirmed the ability of the novel strategy to significantly increase thermal performance which makes thermal energy storage using PCM an effective option for SAHs. Maurya *et al.,* [30] in their study, proposed a new design based on a novel absorber that improves the efficiency of heat transfer and collection. This design uses a tubular surface composed of three counterflow passages made of thin sheet aluminum. Their results showed clearly superior hydraulic thermal performance with a maximum increase in thermal efficiency reaching 60.04%.

Obviously, the researchers have done much work on increasing the absorber area with a least increasing in pressure drop. However, most of the suggested techniques used to increase the surface area leads to significant increment in the power required to push the air through the collector. The innovative idea of using a matrix of longitudinal pipes is a promising solution to deal with that problem with a possibility of maintaining the pressure drop within a reasonable slight increase.

This research is a comparative study of two SAHs that are identical in dimensions and measurements and differ only in the design of the absorber plate. The first is a conventional solar air heater that has a flat absorber plate FPSAH while the second is a novel design uses an array of circular metal tubes arranged longitudinally adjacent to each other in the direction of airflow, which is called a tubular solar air heater array (MTSAH). Performance metrics, encompassing energy gain, loss, pressure drop, and efficiency, are compared between the two systems. The testing phase includes three specific mass flow rates: 0.07 kg/s, 0.05 kg/s, and 0.03 kg/s.

2. Experimental Work Setup Construction

To experimentally examine the thermal characteristics of the SAHs and to make a comparative analysis of their thermal performance (efficiency, outlet air temperature, energy gain, energy loss, pressure drop, etc.), two test setups were built based on ASHRAE standards while the dimensions follow the most conventional solar air heaters sizes [31]. These setups share identical dimensions, materials, and design, differing only in the absorber plate used. These two identical SAHs were installed on the building's roof. The building is in Baghdad/Iraq (latitude is 33.3°N and longitude is 44.4°E). A standard flat aluminium plate was used to construct the first SAH, while straight Aluminium tubes were collected beside each other in a matrix form placed in the direction of airflow to shape the second SAH. Figure 1(a) exhibits a front-view image of the experimental setups for the two SAHs, while Figure 1(b) depicts the arrangement of the experimental setup for the MTSAH. The two top-open SAHs, as visually presented in Figure 1(a), were primarily constructed using rectangular wooden boxes measuring 10 mm in thickness and having dimensions of (1500 x 750 x 80) mm for the frames. Also, the backside of each SAH was fabricated from 10 mm thick plywood (8). A white Polystyrene board (6) of 10 mm was used beneath the absorber plate as an insulator to reduce the heat losses. The rectangular cross-section SAHs having an inlet port (1) at the bottom and outlet port (5) at the top for passing the outside air. Each SAH features a glass cover (2) measuring 150 cm by 75 cm with a thickness of 3 mm positioned at the top of the frame. The design idea of both SAHs is flexible so that the gap between the glass cover and aluminium absorber plate (3) can be changed. Nevertheless, in the present study, the gap from the glass cover of the SAH to the absorber plate was specified at 5 cm. In addition, the structure design of both SAHs can use a double glass cover but the presented results of the current experimental study are for a single glass cover with 3 mm thickness.

A 150 cm by 75 cm aluminium absorber plate with a thickness of 1 mm mounted in the frame beneath the glass cover was used in the FPSAH. To improve the absorber plate's efficiency of the SAH it was painted by dark black colour of high thermal conductivity on both sides. This was to an increase the absorbance of the aluminium absorber plate and tubes from the incident solar-radiation energy required to warm the air.

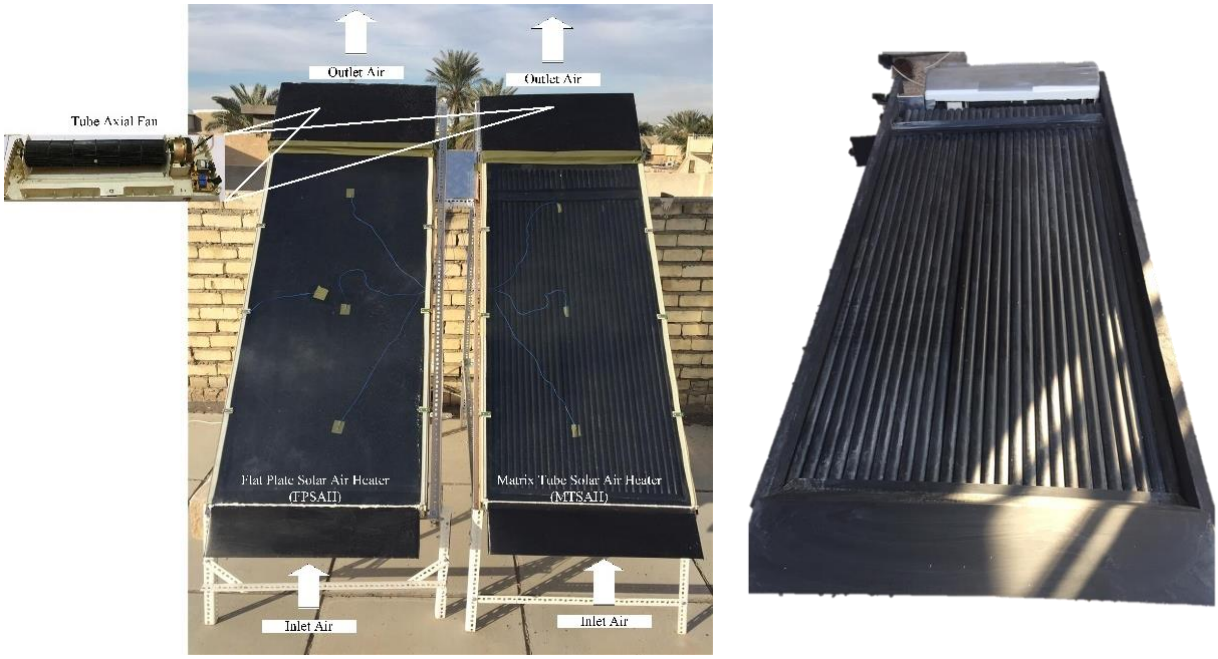

(a) (b)

Fig. 1. The experimental setup, (a) test rig, (b) the absorber of the MTSAH

The inlet and outlet airflow distribution inside the SAH is highlighted and presented schematically in Figure 2. Two identical direct drive tube axial fan (4) was installed at the outlets of each SAH to ensure homogeneous airflow distribution over the absorber plate and low-pressure drop. The airflow rates from these tube axial fans are controlled by a single-phase digital display variac transformer. A vane-type anemometer was used to measure air velocities at the outlet port of each SAH. To determine the average airflow velocity value in the cross-sectional area at the duct's exit, five test locations were used in accordance with Heydari and Mesgarpour [26] recommendations. The specifications of the measurement instruments employed in the present experimental tests are provided in Table 1. A 12-channel temperature data logger equipped with an SD card was employed for data recording. It had been configured to capture data at five-minute intervals. Then these data can be downloaded to open with an Excel sheet. The pressure drop across SAHs was measured by a digital pressure gauge which has a dual channel that can simultaneously detect the pressure difference between two detection ports.

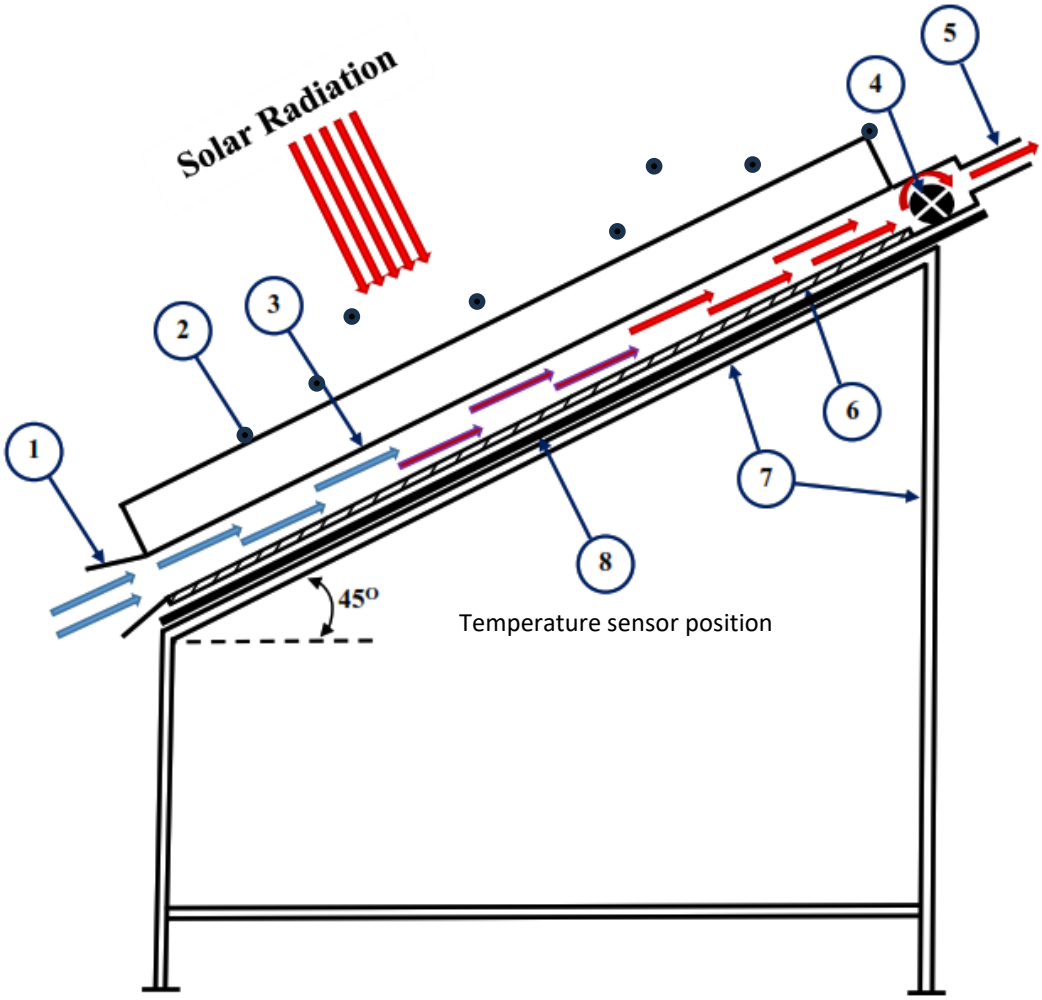

Inlet port (1), glass cover (2), Absorber plate (3), Tube axial fan (4) Outlet port (5), Polystyrene board (6), Stand (7), Wooden frame (8).

Fig. 2. Schematic diagram of the experimental arrangement

The MTSAH absorber made up of aluminium pipes of circular cross-section as stated in Figure 1(b). The aluminium pipe is 150 cm in length with a diameter of 2.5 cm and a wall thickness of 0.1 cm. The outer surfaces of the aluminium pipes were coated with black paint like that used for painting the flat absorber plate to absorb as much of the Solar's heat as possible and to enhance their absorptivity to the solar radiation. All aluminium pipes were collected horizontally with each other in matrix form to ensure good contact by using two aluminium sheets jointed to the absorber tubes. To make an accurate comparison performance study between the two collectors, the space between the glass cover and the upper surface of the pipes (absorber) is kept having the same (5 cm) value which is like the space between the glass cover and the absorber of the FPSAH. Slotted angle steel bar (7) assembled and used to carry the SAHs which having an inclination angle of 45° (latitude of Baghdad city). To receive the largest amount of solar energy during the experimental measurements the two SAHs are orientated to the south direction. Table 1 comprises the technical details pertaining to SAHs.

Table 1
Technical properties of SAH components

Components	Features
Wooden Box	rectangular frame 10 mm thick (1500 x 750 x 80) mm
Glass	low ironed-tempered glass, 3 mm thickness (150 x 75) cm, and the transmittance of 90%.
Absorber plates	Aluminum plate measuring 150 cm by 75 cm with a thickness of 1 mm Aluminum pipes length of 150 cm, Ø=2.5 cm, thickness 0.1 cm.
Absorber coating	Standard dark black paint, the paint absorptivity: 94-95%.
Insulation	Polystyrene board of 10 mm thickness
Fans	Direct drive tube axial fan 40W, 220V, 50HZ, 0.153A ,1300 r/min
Speed control	TDGC2-0.5KVA AC Variable Digital Voltage Adjustable Regulator Transformer 2A 500w 220v Single-phase 0-250V Power Supplies

2.1 Measured Values

Many values are measured and recorded from 8:00 AM to 5:00 PM during the experimental measurements test. All test measurements were conducted through three days 8/3/2023, 10/3/2023, and 13/3/2023. To reduce the effect of the solar intensity changing and the impact of ambient conditions, each experimental test was repeated three times to evaluate its repeatability.

The temperature sensor points for the test rig are shown in Figure 1. Air temperatures are monitored at various positions on the solar air heaters, as illustrated in Figure 3, with corresponding locations for both SAHs being identical and recorded using temperature thermocouples (T-type). Two temperature sensors for measuring air temperatures at the inlet port and outlet port for each SAH, temperature sensors for the surface temperature of glass cover, a temperature thermocouples sensor for measuring the absorber plate surface temperature, and a temperature thermocouples sensor for the back surface temperature of the SAH box. The surface temperatures of the absorber plate were recorded at three positions diagonally of the absorber. Equal spacing (50 cm) with longitudinal centerlines was used to locate the positions of thermocouples for recording the temperature of the absorber plate and glass cover. It is noteworthy to point out that the temperature of the absorber plate for each one of the two SAHs was measured as the average reading of the three thermocouples locating at different points. Moreover, the outside air temperature was measured by using one thermocouple sensor. A pyranometer was used to record the solar radiation intensity at time intervals of five minutes. These readings, along with the readings of the temperature data logger, were saved electronically on the memory cards attached to the devices.

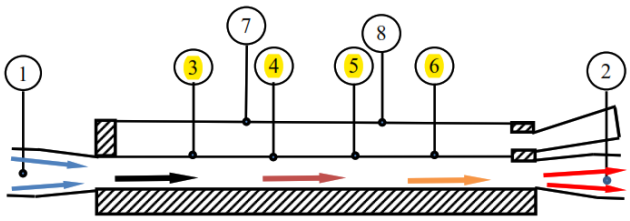

Fig. 3. The temperature sensor's locations

3. Experimental Procedure

The process of doing the experiments include several steps which had been followed

i. Preparations: Some of procedures had been taken before doing beginning of the experiment to conform the different parts readiness include checking of the glass of the cover and cleaning it with some suitable materials to ensure its cleanliness to allow maximum

permeability of the solar radiation. The thermal insulation also was checked to ensure its validity.

ii. Instruments Validation: Careful evaluation was performed to ensure the operational accuracy of all measuring instruments, including pyranometer, U-shaped manometer, voltmeter, ammeter, thermocouples, and data logger.

iii. Operating Procedures: The blower was operated to initiate airflow, and the flow valve had been controlled to precisely adjust the desired airflow rate into the duct. This process ensured uniform and regulated air velocity throughout the system.

iv. Data Collection: Throughout the time of the experiments, various fundamental parameters were regularly recorded. The important parameters which had been focused on include Intensity of solar radiation, air temperatures at the collector's inlet and outlet, ambient temperature, absorber plate temperatures at selected locations, and airflow rates between the collector's inlet and outlet. All measurements were recorded when the system reached a quasi-steady state condition, to ensure the accuracy and reliability of the recorded data.

v. Interval measurements: The above procedures were repeated in regular time steps of 30 minutes, beginning from 8:00 AM to 5:00 PM. This periodic data collection allowed for the evaluation of temporal changes that occurred in system performance throughout the studied period.

vi. End of workday preparations: At the end of a full day's data collection, SAH systems were resettled to the conditions they were in at the beginning of the day. This includes ensuring the glass cover is clean and ensuring proper insulation of all system components to prevent heat loss or leakage, then repeated the same procedures starting from 1 to start collecting data for the next new day.

This carefully planned experimental procedure ensures that reliable data were systematically obtained, which made it easy to comprehensively be evaluated the performance of the SAH system under different conditions.

4. Equations of the Results Parameters

The total heat incident Q_t (W) on the absorber plate of the SAH can be estimated by

$$\mathbf{Q_t} = \boldsymbol{IA_{abs}} \tag{1}$$

where I is the solar intensity (W/m^2) and A_{abs} is the absorber surface area (m^2). Considering T_{out} (°C) is the temperature of the outlet air exit from the SAH, and T_{in} (°C) is the temperature of the air enter SAH, then the total heat gain Q_g (W) can by calculated by Abo-Elfadl *et al.,* [32]

$$\boldsymbol{Q_g} = \boldsymbol{\dot{m}c_p(T_{out} - T_{in})} \tag{2}$$

The mass flowrate of the air enters the SAH denoted by $\dot{m}$ (kg/m^3), can be determined by [28]

$$\boldsymbol{\dot{m} = \rho V A_{in}} \tag{3}$$

where ρ is the density of the air entering the SAH (m^3), V is the average velocity of the air across the entrance of the SAH (m/s), A_{in} is the entrance area (m^2), and c_p is the specific heat of the air (j/kg.K), then, the solar air heater efficiency is given by Hassan *et al.,* [33]

$$\boldsymbol{\eta = \frac{Q_g}{Q_t}} \tag{4}$$

To find Q_L (W) which represent the top surface heat losses the following formula can be used [34]

$$\boldsymbol{Q_L = \frac{(T_c - T_a)}{\frac{1}{A_c h_c + A_c h_r}}} \tag{5}$$

where T_c (°C) and T_a (°C) are the average temperature of the glass cover and ambient air respectively, A_c (m^2) is the glass cover area, h_c (W/m^2) is the convective heat transfer coefficient of the glass cover and h_r (W/m^2) is the radiation heat transfer coefficient on the top of the glass cover.

To determine h_c and h_r the following equations can be used respectively [27,35]

$$\boldsymbol{h_c = 5.7 + 3.8\, V_w} \tag{6}$$

$$\boldsymbol{h_r = \frac{\sigma \varepsilon_c (T_c + T_s)(T_c^2 + T_s^2)(T_c - T_s)}{(T_c + T_a)}} \tag{7}$$

where V_w is the speed of the wind (m/s), ε_c is the emissivity of the glass cover, s is the Stefan-Boltzmann coefficient (5.667×10^{-8}) W/m^2. K^4, T_s is the sky temperature and T_a is the ambient temperature.

5. Uncertainty and Error Analysis

When conducting any experiment and recording data, it is inevitable that there will be some errors resulting from inaccuracy which is called “uncertainty” [36]. In this experimental study, the experimental errors and the uncertainty associated with measuring devices have been considered. Moreover, calibration procedures have been conducted for the sensors used, including thermocouples and pressure measuring devices. To minimize measurement errors, various precautions have been used, such as insulating the point junction of the thermocouple to solely measure surface temperature. As such, the measurements under the same conditions were conducted at least three times to identify the data closest to the true value and adopt it. The results presented in this work have been corrected based on the outcomes of these calibration procedures. The approach described by Taylor was followed to find errors and analyse uncertainty [37,38]. The following equation is used to determine the uncertainty (d) of a value (f), such as the efficiency (h) of the solar air heater obtained from the experimental data using d_x and d_y which represent the uncertainty of the efficiency at x and y respectively [37]

$$\boldsymbol{\delta = \sqrt{\left(\frac{\partial f}{\partial x}\right)^2 \delta_x^2 + \left(\frac{\partial f}{\partial y}\right)^2 \delta_y^2}} \tag{8}$$

Finally, according to these calculations, it can be estimated that the uncertainty in the useful power is around 1.78, pressure drop is ± 0.32, and for the efficiency is in the range of 1.4% to 2.85%.

6. Results and Discussion

Experiments and measurements were carried out for the period from 8-3-2023 to 13-3-2023, where it was confirmed that the sky was clear and free of clouds. The results are shown for the MTSAH and FPSAH for three air mass flow rates that enters to the SAHs port: 0.03, 0.05, and 0.071 kg/s. The temperatures that are shown in the findings are averages of the values that were measured.

Figure 4 illustrates the diurnal variation in solar intensity observed during the measurement days. It is evident that solar intensity steadily increases in the morning, reaching its zenith between 11:30 AM and 12:30 PM, after which it gradually declines until the conclusion of the observation period. Importantly, it is worth noting that the most substantial discrepancy in solar intensity, recorded across the three measurement days, amounts to merely 2.3%. This marginal disparity does not constitute a meaningful divergence in solar intensity among these days. These findings suggest that the timing of data collection exerts no discernible influence on the resultant outcomes.

Furthermore, results demonstrate a coherent pattern with absorber plate temperatures mirroring the solar intensity trend. These temperatures ascend progressively until approximately noon, subsequently declining towards the end of the data collection period. The time gap between the highest temperature and the peak solar intensity can be explained by the duration needed to heat up the SAHs and the air circulating through them. Significantly, it is observed that absorber plate temperatures surpass ambient air temperatures, elucidating that the air undergoes heating as it traverses through the absorber plate.

Remarkably, all measured temperatures within the SAHs exceed the ambient temperature, in accordance with experimental design. Upon juxtaposing the results presented in Figure 4(a), Figure 4(b), and Figure 4(c) for the FPSAH and the MTSAH at varying air mass flow rates, it becomes apparent that augmenting the mass flow rate within the SAH leads to a reduction in exit air temperatures. The investigation shows that increasing the air mass flow rates within the range of 0.03 to 0.071 kg/s, representing a 133.33% increase, leads to a reduction in absorber plate temperatures. Specifically, for the FPSAH, there is an approximate decline of 12.8%, whereas for the MTSAH, this decrease is notably more substantial, amounting to approximately 28.7%. These observations underscore the heightened sensitivity of absorber plate temperatures in the MTSAH configuration to variations in mass flow rate when compared to the FPSAH configuration. Notably, this outcome can be attributed to the larger surface area of the absorber in the case of the MTSAH compared to the FPSAH. The absorber contact area of the MTSAH is approximately π times larger than that of the FPSAH. Additionally, the tubular absorber in the MTSAH encompasses half of the absorber's total peripheral area, affording a larger exposed surface area to solar radiation than the FPSAH. Furthermore, the unique design of the MTSAH absorber mitigates reflected solar radiation, minimizing top heat loss through internal reflections between the absorber tubes' surfaces. Consequently, the MTSAH exhibits greater heat transfer to the air compared to the FPSAH.

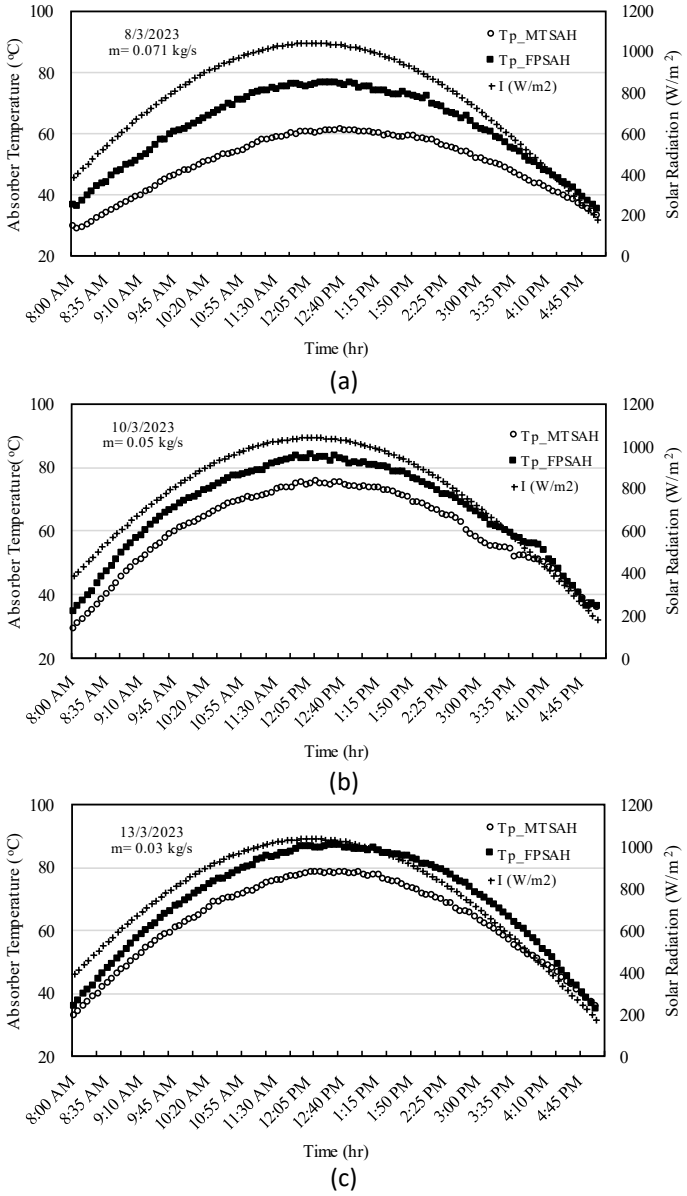

Fig. 4. Daily measurement of absorber plate temperature and solar radiation with time for MTSAH and FPSAH at a different air mass flow rate

Figure 5 depict the temporal evolution of the temperature difference between inlet temperatures (Tin) and outlet temperatures (Tout) for both the FPSAH and the MTSAH. The measurements encompass a spectrum of air mass flow rates, specifically 0.03, 0.05, and 0.071 kg/s. Remarkably, this temperature difference, denoted as (T_{out} - T_{in}), mirrors a consistent pattern akin to that observed for absorber temperature and solar intensity. It steadily increases throughout the day until it reaches its zenith at solar noon (12:00 PM), followed by a gradual decline until sunset.

The distinct thermal performance characteristics of the MTSAH, owing to its superior convective heat transfer efficiency when compared to the FPSAH, become evident as the temperature differences for MTSAH significantly outstrip those of the FPSAH, as illustrated in Figure 5. Furthermore, an insightful observation from the figure is that the temperature difference (T_{out} - T_{in}) diminishes for both FPSAH and MTSAH with increasing air mass flow rates. This phenomenon arises from the reduced residence time of air in contact with the absorber, resulting from the escalated air

input velocity. It is worth noting that increasing in air velocity is normally cause enhancement of the coefficient of heat transfer between the absorber plate and the passing air in any case.

In general, increasing air mass flow rate led to decreasing in temperature difference across the SAH absorber (T_{out} - T_{in}) regardless the kind of the absorber design which may be flat or tubular. This correlation underscores the influence of heightened convection processes, which serve to lower absorber temperatures. Importantly, these temperature differences may potentially impact the overall performance metrics such as the useful power and efficiency of the SAHs.

It is worth noting that a conspicuous and consistent decline in the temperature difference, approximately amounting to 34%, is evident for both collector types across the range of varying mass flow rates. This robust consistency reaffirms the precision and reliability of the experimental results, lending support to the assertion that no significant deviations were introduced by potential variations in measurements on different evaluation days, as previously discussed.

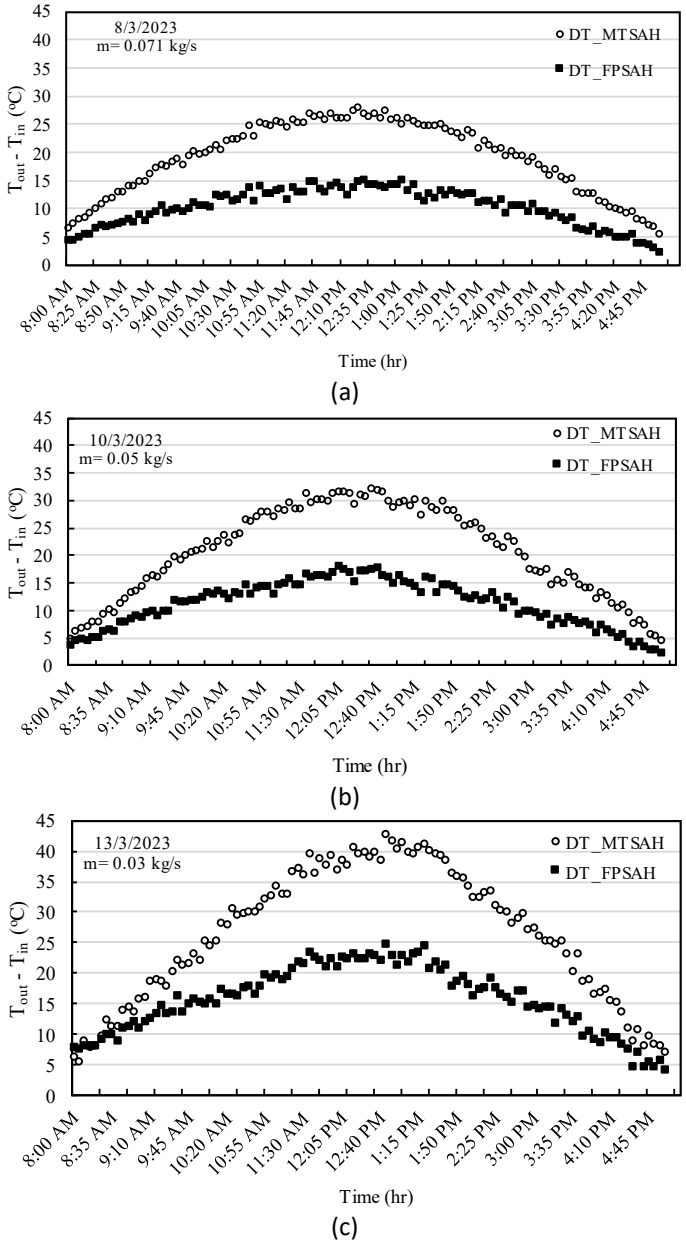

Fig. 5. Daily tracking of inlet and outlet air temperature variation over time for MTSAH and FPSAH at various air mass flow rates

The efficiency of a SAH hinges significantly on its ability to harness solar energy. To assess this, the temporal dynamics of useful power accumulated by the flowing air, a crucial parameter have been examined, as illustrated in Figure 6. The figure presents data for both MTSAH and FPSAH under varying airflow conditions within SAHs. Furthermore, Figure 7 provides a comprehensive depiction of the cumulative evolution of collected useful power over time. Figure 6 highlights a prominent trend where the hourly useful power closely mirrors the variations observed in incoming solar intensity and SAH temperatures. Notably, it exhibits a discernible ascent from the early morning hours, with a notably superior performance of MTSAH compared to FPSAH. This ascent culminates around 12:00 PM, followed by a gradual decline until the culmination of the observation period. This observed correlation can be attributed to the substantial influence of the SAH outlet air temperature on the resultant useful power. In contrast, Figure 7 presents a comprehensive overview of the cumulative useful energy over time, spanning from the initiation of measurements to the conclusion of the data recording period. In this context, MTSAH consistently outperforms FPSAH, demonstrating a clear superiority in terms of total useful energy collected. Figure 6 and Figure 7 jointly underscore an important observation: as the inlet air mass flow rate increases, there is a corresponding augmentation in useful power for both MTSAH and FPSAH. This phenomenon arises from the heightened convective heat transfer coefficient associated with the increased airflow rate. Moreover, the analysis indicates a noteworthy trend: at an air mass flow rate of 0.07 kg/s, the useful power significantly surpasses that observed at 0.03 kg/s for both SAH types. Specifically, in the case of MTSAH, there is a notable 29.7% increase, while FPSAH exhibits a 22.4% increment. However, it is noteworthy that the advantage in useful power at 0.07 kg/s is less pronounced when compared to the results at 0.05 kg/s. For this relatively high mass flow rate value the increase in useful power is 12.3% and 9.26% for MTSAH and FPSAH, respectively. This indicates that the obtained of useful energy rate is decreased with increasing of air mass flow rate, i.e. there are an optimal operation condition of SAH. This is because the enhancement of solar heat gain by SAH absorber is decreases when air flow rate increases as previous research approved [27,32]. So, the results approved that the relation of the useful energy with air velocity is not linear relation, thus increasing mass flow rate is not necessarily mean increasing in the obtained of useful energy. Moreover, at a specified value of air mass flow rate, the useful energy amount will be fixed and doesn't increase even if the air mass flow rate increases.

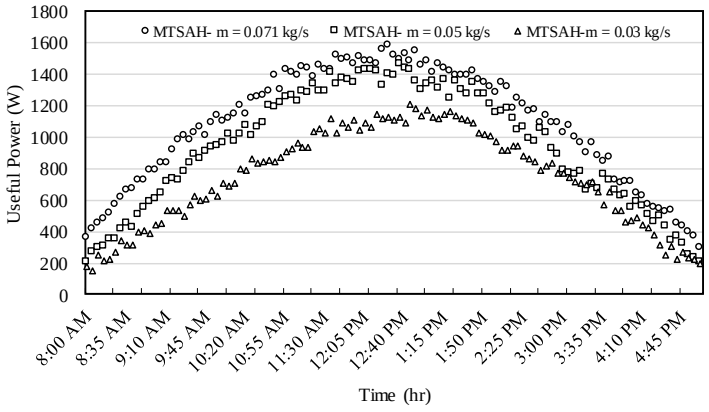

(a)

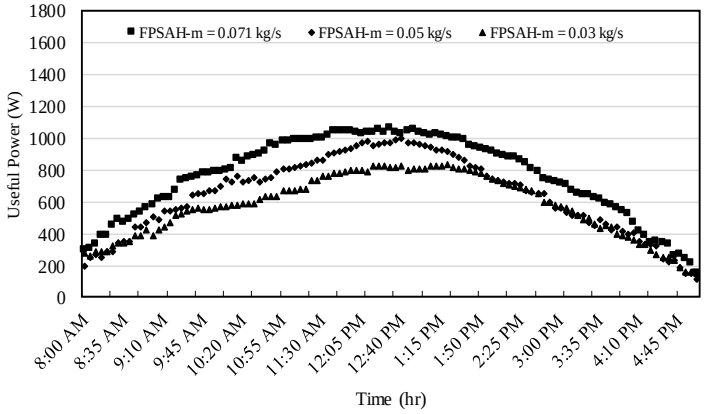

(b)

Fig. 6. Daily variation of the useful power with time for (a) MTSAH and (b) FPSAH at a different air mass flow rate

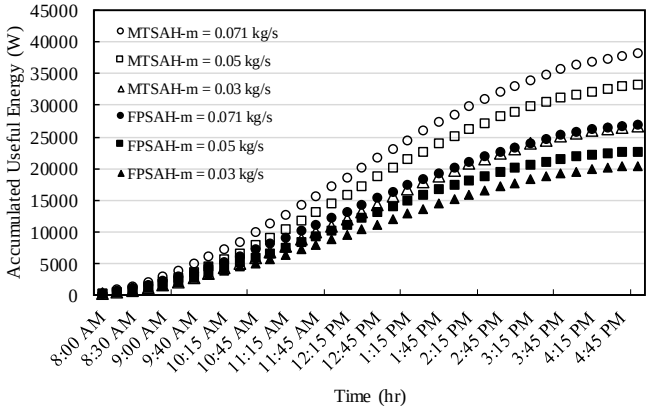

Fig. 7. Daily Fluctuation in accumulated useful energy over time for MTSAH and FPSAH at various air mass flow rates

The efficiency of a SAH hinges significantly on heat dissipation from its upper surface as heat naturally ascends. In Figure 8, it can observe the variations in hourly heat losses from the top surface of SAHs, referred to as "top losses," across different inlet air mass flowrates. Notably, the figure mirrors the hourly changes in both outlet air temperature and overall power gains. Top losses progressively mount in the morning until approximately 11:30 AM, subsequently tapering off. This behavior is closely tied to the temperature of the absorber and glass cover, as they influence the top power losses. Furthermore, it is evident that the top losses in FPSAH configurations are notably higher than those in MTSAH setups, yet these losses decline as the incoming air mass flowrates increases for both SAH types. This correlation clarifies the rationale behind the rise in power gain as inlet air mass flowrates escalates and as previously mentioned, why MTSAH outperforms FPSAH in terms of power gain.

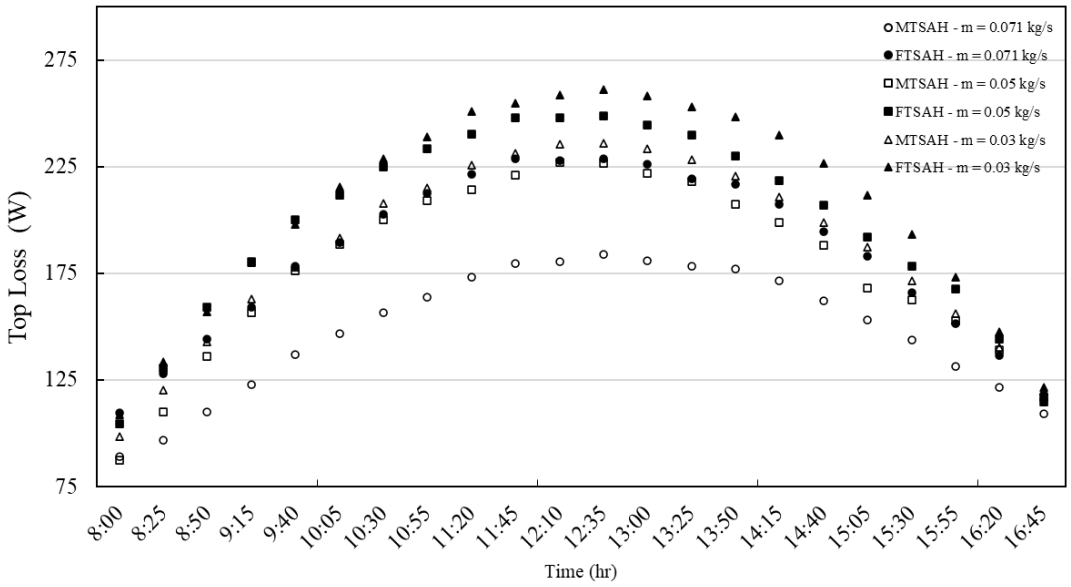

Fig. 8. Daily variation of the top surface losses with time for MTSAH and FPSAH at a different air mass flow rate

Efficiency is a pivotal metric employed to gauge the performance of SAHs and holds significant value as a precursor to studies aimed at enhancing SAH functionality. Figure 9 provides a comprehensive overview of how the efficiency of both the MTSAH and the FPSAH evolves over time under varying intake air mass flow rates.

As delineated in Figure 9, SAH efficiency exhibits a gradual improvement throughout the day, commencing in the morning and concluding in the evening. This enhancement is primarily attributed to the escalating incoming solar energy. Intriguingly, even during periods of declining solar energy input, efficiency experiences an upswing around midday. This phenomenon can be explained by the energy that is stored in the structure of the SAH during morning times when there is abundant in solar energy and then returns to release in the late afternoon, the time of solar radiation decreasing.

Furthermore, a clear trend emerges here as MTSAH consistently outperforms FPSAH at all studied inlet air velocities. This can be explained by the large absorption area of the MTSAH compared to the FPSAH, which allows greater contact with the air and thus compensates for the losses resulting from the top to a greater extent.

Moreover, it is noteworthy that when the velocity of air at the inlet increases, the coefficient of convective heat transfer proportionally rises, leading to increased heat gain. Consequently, this augmentation results in lower absorber temperatures and a subsequent reduction in top losses.

Figure 9 culminates by illustrating the striking disparity in SAH efficiency at peak performance. In the case of MTSAH, the efficiency peaks at a remarkable 92.18% with an inlet air flowrate of 0.071 kg/s. Conversely, FPSAH achieves an efficiency of approximately 61.9% under the same conditions, highlighting the remarkable advantage of MTSAH in harnessing and maximizing solar energy conversion.

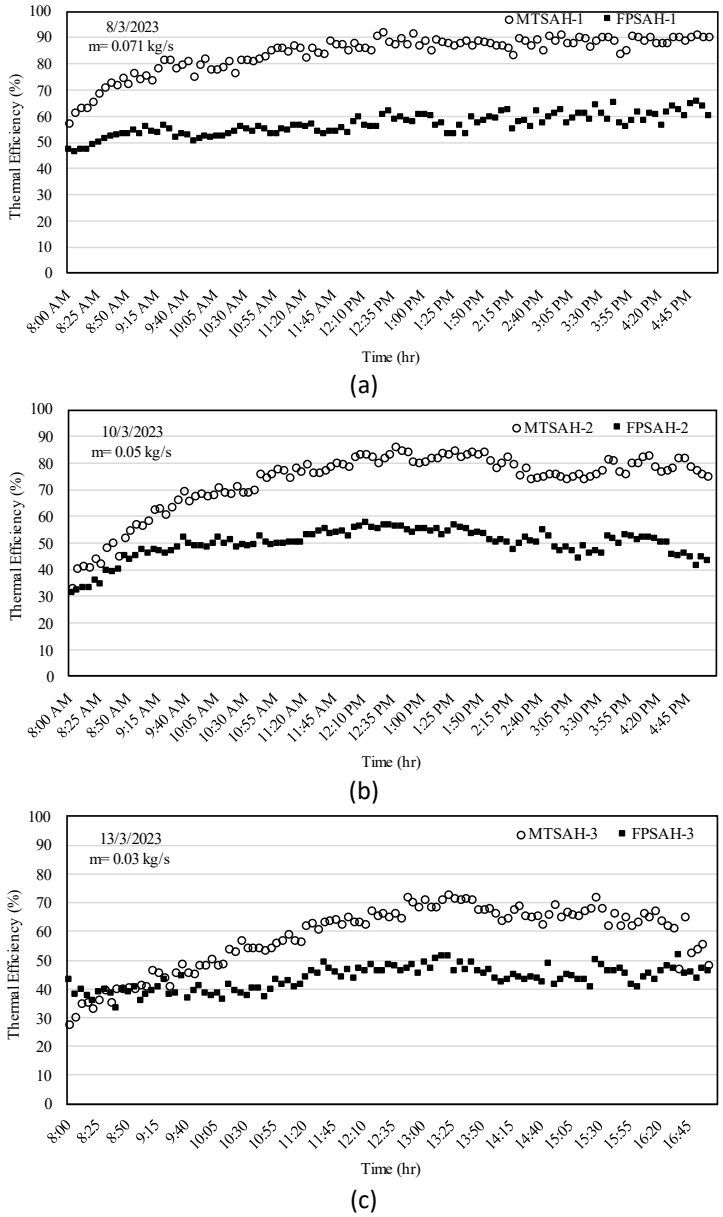

Fig. 9. Daily variation of the SAH efficiency with time for MTSAH and FPSAH at a different air mass flow rate

Evaluating the efficiency of a SAH involves considering the pressure drop resulting from airflow resistance, which is a key parameter. When factoring in the energy consumed by the blower, it's essential to note that an increased pressure drop can diminish the net useful energy because more power is consumed by the blower. In Figure 10, it can observe the pressure drop across the SAHs at various inlet air velocities. This figure illustrates that the pressure drop across the MTSAH is greater than that of the FPSAH. Furthermore, in general, the pressure drop through the SAHs escalates as the inlet air mass flowrate increases. Notably, for inlet air mass flowrates of 0.071 kg/s, 0.05 kg/s, and 0.03 kg/s, the pressure drop through the SAH increases by approximately 30%, 21%, and 6%, respectively.

An intriguing finding can be seen by looking more closely at the data in Figure 7 and Figure 10. The striking agreement between these figures suggests that the pressure drop has no impact on the output of usable power. This is mainly because the pressure drop values are comparatively small in relation to the output useful power generated by the SAHs.

Obviously, the enhancement in the received solar energy and so increasing in the useful energy is due to the increasing in the surface area of the absorber plate of the SAH. Despite that it neither effectively raises the pressure drop inside the system nor increases the power required to run the blower and pump the air. This very important conclusion indicates that despite the great enhancement in the heat gained from this modification there will be no more loads that should be added like pressure increasing or high required pumping energy. In other words, the modification successfully increases the thermal energy of SAH without any considerable losses in the thermal or hydraulic performance of the system. In essence, these findings suggest that while pressure drop does increase with higher inlet air velocities, it doesn't significantly affect the overall useful power output of the SAHs. This insight can be valuable in optimizing the design and operation of such solar air heating systems.

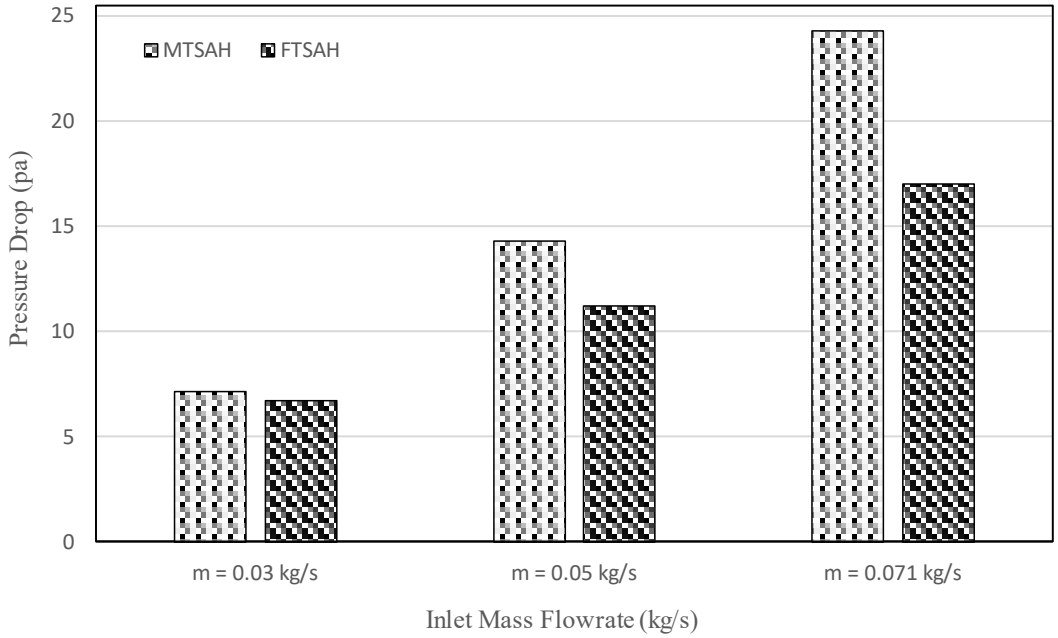

Fig. 10. Pressure drop for MTSAH and FPSAH at a different air mass flow rate

7. Conclusion

Using a matrix of longitudinal pipe as absorbing area instead preferred over flat plate is the main novelty of the work. The experimental investigation of the performance of the novel tubular SAH absorber design, denoted as MTSAH, across a spectrum of inlet air mass flow rates is a central focus of this study. The most important conclusions reached by the experiments of the research study can be summarized as follows

i. In direct comparison, the performance of MTSAH is evaluated against that of the conventional FPSAH. The comprehensive findings unequivocally demonstrate that MTSAH consistently outperforms FPSAH across various inlet air flow rates regarding heat gain, outlet air temperature, and overall efficiency.
ii. MTSAH exhibits a noteworthy advantage, manifesting in a maximum increase in the air temperature difference between outlet and inlet temperatures by 46.5°C at inlet air mass flow rate of 0.03 kg/s, while it 45.4°C at inlet air mass flow rate of 0.05 kg/s, and 46.4°C at inlet air mass flow rate of 0.071 kg/s, when compared to FPSAH.
iii. MTSAH significantly augments daily useful power by approximately 29.71% for inlet air mass flow rate of 0.03 kg/s, however it 38.23% for inlet air mass flow rate of 0.05 kg/s, and 43.1%

for inlet air mass flow rate of 0.071 kg/s, in comparison to FPSAH. These findings firmly establish the superior performance of MTSAH in relation to previously presented SAH designs.

iv. The heightened efficiency of this innovative SAH design, coupled with its cost-effective materials, and lower maintenance requirements, underscores the immense promise of investing in solar air heating technology. Future investigations could explore enhancements such as dual solar air paths and the utilization of heat transfer enhancers like porous media, among other avenues.

v. While increasing the air mass flow rate amplifies convective heat transfer and useful power, it does not yield a linear increase in efficiency. This insight suggests the potential for reaching peak efficiency at a specific air mass flow rate.

vi. The MTSAH design presents a compelling case for the advancement of SAH efficiency and effectiveness, laying the foundation for further exploration aimed at optimizing SAH designs and operational parameters to enhance energy capture and utilization.

Author Contributions

Munther Abdullah Mussa Modeling, Original draft Preparation, Writing - Reviewing and Editing Issam M. Ali Aljubury carried out the experiments and Sarmad Abdul-Razzaq Rashid contributed to the final version of the manuscript. Munther Abdullah Mussa supervised the project.

References

[1] Sadiq, Hassan Hadi, and Munther Abdullah Mussa. "Experimental Study of Thermal Conductivity Effect on the Performance of Thermal Energy Storage." *Jordan Journal of Mechanical & Industrial Engineering* 16, no. 4 (2022).

[2] Zaraa Allah, Mohammad, Azian Hariri, and Haslinda Mohamed Kamar. "Comparison of Thermal Comfort Condition of Naturally Ventilated Courtyard, Semi-Outdoor and Indoor Air-Conditioned Spaces in Tropical Climate." *Journal of Advanced Research in Fluid Mechanics and Thermal Sciences* 101, no. 1 (2023): 45-58. https://doi.org/10.37934/arfmts.101.1.4558

[3] Kinan, A., and N. A. Che Sidik. "Experimental studies on small scale of solar updraft power plant." *Journal of Advanced Research Design* 22, no. 1 (2016): 1-12.

[4] Atiyah, Ayad, Yaser Alaiwi, Mohammed Hussein Radhi, and Ahmad Jundi. "Numerical Analysis for Enhanced Water Desalination in Solar Stills with Optimized Glass Cover Angles." *Journal of Advanced Research in Numerical Heat Transfer* 22, no. 1 (2024): 31-45. https://doi.org/10.37934/arnht.22.1.3145

[5] Ghaderian, J., C. S. Nor Azwadi, and H. A. Mohammed. "Modelling of energy and exergy analysis for a double-pass solar air heater system." *Journal of Advanced Research in Fluid Mechanics and Thermal Sciences* 16, no. 1 (2015): 15-32.

[6] Farhan, Ammar A., Hamdi E. Ahmed, and Munther A. Mussa. "Thermal-hydraulic performance of a V-groove solar air collector with transverse wedge-shaped ribs." *Arabian Journal for Science and Engineering* 47, no. 7 (2022): 8915-8930. https://doi.org/10.1007/s13369-021-06442-5

[7] Saxena, Abhishek, Erdem Cuce, Desh Bandhu Singh, Muneesh Sethi, Pinar Mert Cuce, Atul A. Sagade, and Avnish Kumar. "Experimental studies of latent heat storage based solar air heater for space heating: A comparative analysis." *Journal of Building Engineering* 69 (2023): 106282. https://doi.org/10.1016/j.jobe.2023.106282

[8] Ellis, Joseph, Richard Opoku, Charles K. K. Sekyere, and Albert K. Arkoh. "Solar crop dryer with thermal energy storage as backup heater." *Solar Compass* 8 (2023): 100058. https://doi.org/10.1016/j.solcom.2023.100058

[9] El-Bialy, E., and S. M. Shalaby. "Recent developments and cost analysis of different configurations of the solar air heaters." *Solar Energy* (2023): 112091. https://doi.org/10.1016/j.solener.2023.112091

[10] Xiao, Hui, Zhimin Dong, Zhichun Liu, and Wei Liu. "Heat transfer performance and flow characteristics of solar air heaters with inclined trapezoidal vortex generators." *Applied Thermal Engineering* 179 (2020): 115484. https://doi.org/10.1016/j.applthermaleng.2020.115484

[11] Kalogirou, Soteris A. "Solar thermal collectors and applications." *Progress in Energy and Combustion Science* 30, no. 3 (2004): 231-295. https://doi.org/10.1016/j.pecs.2004.02.001

[12] Farhan, Ammar A., Zain Alabdeen H. Obaid, and Sally Q. Hussien. "Analysis of exergetic performance for a solar air heater with metal foam fins." *Heat Transfer* 49, no. 5 (2020): 3190-3204. https://doi.org/10.1002/htj.21769

[13] Alaskari, Mustafa, Arwa M. Kadhim, Ammar A. Farhan, Moustafa Al-Damook, and Mansour Al Qubeissi. "Performance Evaluation of Roughened Solar Air Heaters for Stretched Parameters." *Clean Technologies* 4, no. 2 (2022): 555-569. https://doi.org/10.3390/cleantechnol4020034
[14] Farhan, Ammar A., and Hana Abdulhussien Sahi. "Energy analysis of solar collector with perforated absorber plate." *Journal of Engineering* 23, no. 9 (2017): 89-102. https://doi.org/10.31026/j.eng.2017.09.07
[15] Fudholi, Ahmad, and Kamaruzzaman Sopian. "Review on exergy and energy analysis of solar air heater." *International Journal of Power Electronics and Drive Systems* 9, no. 1 (2018): 420. https://doi.org/10.11591/ijpeds.v9.i1.pp420-426
[16] Mahdi, Ali Hammoodi, and Munther Abdullah Mussa. "Comprehensive review of optimization of latent thermal energy storage systems using multiple parameters." *Journal of Energy Storage* 86 (2024): 111120. https://doi.org/10.1016/j.est.2024.111120
[17] Kadhim, Arwa M., Mena S. Mohammed, and Ammar A. Farhan. "Impact of Discrete Multi-arc Rib Roughness on the Effective Efficiency of a Solar Air Heater." *Jordan Journal of Mechanical & Industrial Engineering* 16, no. 4 (2022).
[18] Theeb, Ali H., and Munther A. Mussa. "Numerical investigation on heat transfer enhancement and turbulent flow characteristics in a high aspect ratio rectangular duct roughened by intersecting ribs with inclined ribs." *Journal of Engineering* 26, no. 5 (2020): 20-37. https://doi.org/10.31026/j.eng.2020.05.02
[19] Anas, Rusul Qusay, and Munther Abdullah Mussa. "Maximization of heat transfer density from a single-row cross-flow heat exchanger with wing-shaped tubes using constructal design." *Heat Transfer* 50, no. 6 (2021): 5906-5924. https://doi.org/10.1002/htj.22155
[20] Aljubury, Issam Ali, Mohammed Khalil Hussain, and Ammar Farhan. "The optimal geometric design of a v-corrugated absorber solar air heater integrated with twisted tape inserts." *Journal of Thermal Engineering* 9, no. 2 (2021): 478-496.
[21] Jain, Sheetal Kumar, Ghanshyam Das Agrawal, and Rohit Misra. "A detailed review on various V-shaped ribs roughened solar air heater." *Heat and Mass Transfer* 55, no. 12 (2019): 3369-3412. https://doi.org/10.1007/s00231-019-02656-4
[22] Misra, Rohit, Jagbir Singh, Sheetal Kumar Jain, Sachin Faujdar, Muskan Agrawal, Arin Mishra, and Pradeep Kumar Goyal. "Prediction of behavior of triangular solar air heater duct using V-down rib with multiple gaps and turbulence promoters as artificial roughness: a CFD analysis." *International Journal of Heat and Mass Transfer* 162 (2020): 120376. https://doi.org/10.1016/j.ijheatmasstransfer.2020.120376
[23] Taha, Safa Y., and Ammar A. Farhan. "Performance augmentation of a solar air heater using herringbone metal foam fins: An experimental work." *International Journal of Energy Research* 45, no. 2 (2021): 2321-2333. https://doi.org/10.1002/er.5927
[24] Omotosho, Emmanuel, and Philip Hackney. "Performance prediction of single-pass and multi-pass low-cost solar air heater." *Thermal Science and Engineering Progress* 47 (2024): 102322. https://doi.org/10.1016/j.tsep.2023.102322
[25] Pachori, Himanshu, Prashant Baredar, Tanuja Sheorey, Bhupendra Gupta, Vikas Verma, Katsunori Hanamura, and Tushar Choudhary. "Sustainable approaches for performance enhancement of the double pass solar air heater equipped with energy storage system: A comprehensive review." *Journal of Energy Storage* 65 (2023): 107358. https://doi.org/10.1016/j.est.2023.107358
[26] Heydari, Ali, and Mehrdad Mesgarpour. "Experimental analysis and numerical modeling of solar air heater with helical flow path." *Solar Energy* 162 (2018): 278-288. https://doi.org/10.1016/j.solener.2018.01.030
[27] Hassan, Hamdy, Saleh Abo-Elfadl, and M. F. El-Dosoky. "An experimental investigation of the performance of new design of solar air heater (tubular)." *Renewable Energy* 151 (2020): 1055-1066. https://doi.org/10.1016/j.renene.2019.11.112
[28] Abo-Elfadl, Saleh, Mohamed S. Yousef, and Hamdy Hassan. "Energy, exergy, and enviroeconomic assessment of double and single pass solar air heaters having a new design absorber." *Process Safety and Environmental Protection* 149 (2021): 451-464. https://doi.org/10.1016/j.psep.2020.11.020
[29] Hedau, Ankush, and S. K. Singal. "Study on the thermal performance of double pass solar air heater with PCM-based thermal energy storage system." *Journal of Energy Storage* 73 (2023): 109018. https://doi.org/10.1016/j.est.2023.109018
[30] Maurya, Om Kapoor, Jasinta Poonam Ekka, Dhananjay Kumar, Disha Dewangan, and Adarsh Singh. "Experimental and numerical methods for the performance analysis of a tubular three-pass solar air heater." *Energy* 283 (2023): 128640. https://doi.org/10.1016/j.energy.2023.128640
[31] Dheyab, Hussam S., Manar Salih Mahdi Al-Jethelah, Tadahmun Ahmed Yassen, and Thamir Khalil Ibrahim. "Experimental study of the optimum air gap of a rectangular solar air heater." *Journal of Advanced Research in Fluid Mechanics and Thermal Sciences* 59, no. 2 (2019): 318-329.

[32] Abo-Elfadl, Saleh, Mohamed S. Yousef, M. F. El-Dosoky, and Hamdy Hassan. "Energy, exergy, and economic analysis of tubular solar air heater with porous material: an experimental study." *Applied Thermal Engineering* 196 (2021): 117294. https://doi.org/10.1016/j.applthermaleng.2021.117294
[33] Hassan, Hamdy, Osman Omran Osman, and Mahmoud N. Abdelmoez. "Energy and exergy evaluation of new design nabla shaped tubular solar air heater (∇ TSAH): Experimental investigation." *Energy* 276 (2023): 127451. https://doi.org/10.1016/j.energy.2023.127451
[34] Kumar, P. Ganesh, K. Balaji, D. Sakthivadivel, V. S. Vigneswaran, M. Meikandan, and R. Velraj. "Effect of using low-cost thermal insulation material in a solar air heating system with a shot blasted V-corrugated absorber plate." *Thermal Science and Engineering Progress* 14 (2019): 100403. https://doi.org/10.1016/j.tsep.2019.100403
[35] Ansari, Mohammad, and Majid Bazargan. "Optimization of flat plate solar air heaters with ribbed surfaces." *Applied Thermal Engineering* 136 (2018): 356-363. https://doi.org/10.1016/j.applthermaleng.2018.02.099
[36] Fathi, Mohammed Ibrahim, and Munther Abdullah Mussa. "Experimental study on the effect of tube rotation on performance of horizontal shell and tube latent heat energy storage." *Journal of Energy Storage* 39 (2021): 102626. https://doi.org/10.1016/j.est.2021.102626
[37] Taylor, John R. *An Introduction to Error Analysis: The Study of Uncertainties in Physical Measurements*. University Science Books, 1997.
[38] Holman, Jack. *Experimental Methods for Engineers*. McGraw-Hill, 2012.